Journal of Harbin Engineering University
ISSN: 1006-7043

Vol 44 No. 12
December 2023

Modelling and Simulation of a Photovoltaic Pumping System Using an Asynchronous Motor Controlled by the PWM Technique

Moulay Fatima [1], Habbati Assia [2]

[1] University of Technology, University of Djillali Liabés, Irecom Laboratory,Sidi bel abbes, Algeria
[2] University of Technology , Energarid Laboratory,Bechar, Algeria

Abstract

Today, the exploitation of photovoltaic energy offers an inexhaustible supply of energy but above all clean and non-polluting energy, and due to the increase in electricity costs, photovoltaic solar pumping systems have become a good solution, especially in rural areas, which is a definite advantage. These have had a large share in photovoltaic energy application projects and they belong today to the most significant applications of photovoltaic energy. This work presents an autonomous photovoltaic water pumping system driven by an asynchronous motor.

First, a modelling of all the components of the pumping system chain is made, second, and to improve the performance of the system, we detail the technique disturb and observe (P&O) which makes it possible to understand how we can achieve a system with less oscillations and greater efficiency when monitoring the maximum power point of the PV panel for variations metrology and the use of the MPPT technique.

Then, the converter is combined with a voltage source inverter to convert direct current to alternating current to power the asynchronous motor, to operate the centrifugal pump. Finally, a simulation of the assembly is made using the MATLAB Simulink platform and the set of results are of great importance for the management of this type of installation.

Keywords: AC motors, Charge-pumping, DC-DC power converters, Maximum power point trackers, Photovoltaic systems.

1. Introduction

The energy needs of industrialized societies are constantly increasing. Moreover, emerging countries will need more and more energy to carry out their development [1].

The systematic use of fossil fuels, such as oil, coal and natural gas are the most widespread for the production of electricity, makes it possible to have low production costs but leads to a massive release of polluting gas. Thus, the electricity production from these fuels is the source of 40% of global CO_2 emissions [2]. Renewable energies offer the possibility of producing electricity cleanly and above all with less dependence on resources, on condition of accepting their natural fluctuations [3].

A photovoltaic pump basically comes in two ways depending on whether it works with or without a battery. While the first uses a battery to store the electricity produced by the photovoltaic modules, the battery-less pump "pump over the sun" uses a tank to store water until it is used. In this general context, our work focuses on the study and simulation of a photovoltaic pumping system without battery "pump over the sun". This pumping system is a practical and economical solution to the problem of lack of water especially in desert regions [4].

First, we will present a general approach on the photovoltaic energy. Second, we will establish the modelling of a photovoltaic generator and the various components of the photovoltaic pumping system and then, we will present the MPPT method then the simulation and the interpretation of the results. We will end our work with a conclusion.

This paper presents the analysis, modelling and control model of the electrical part of a PV generation system using a boost converter, connected to an asynchronous motor which supplies a centrifugal pump illustrated by the synoptic diagram given in Fig.1.

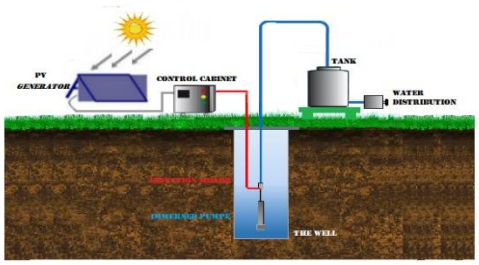

Fig. 1. Synoptic diagram of the PV system

2. Description And Modelling Of The System

Figure 2, shows the block diagram of PV module with boost converter for water pumping application, consisting of the following five blocks: Photovoltaic module; boost converter; PWM inverter PWM; Three-phase asynchronous motor and centrifugal pump.

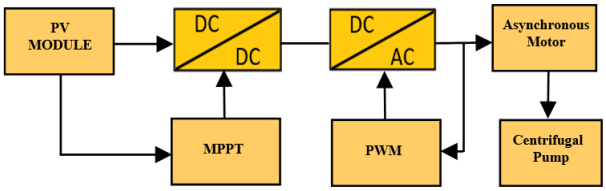

Fig. 2. Block diagram of MPPT based PV module with Boost converter for water pumping application

The PV module produces a low DC output voltage which will be amplified with a Boost converter and since the output of the PV generator varies, an MPPT algorithm is used to track the maximum power of the PV module [5].

Here, the Perturb and Observe (P&O) algorithm is used due to its simplicity and ease of implementation. Power and current are taken as input to the P&O algorithm. By analysing power and current variations, a corresponding duty cycle is produced. This duty cycle signal is given as a gate signal for the boost converter. The amplified output DC voltage is converted into a three-phase AC signal using a PWM inverter. The inverter output voltage (380V) is given to the motor to drive the centrifugal pump [6]

2.1 PV generator model

A photovoltaic generator (GPV) or module consists of a set of elementary photovoltaic cells, connected in series and/or parallel in order to obtain satisfactory electrical characteristics such as power, short-circuit current or circuit voltage open. To find the model of the photovoltaic generator (GPV), you must first find the equivalent electrical circuit [7].The photovoltaic cell is also represented by the "standard" model with a single diode. This model has a as shown in Fig. 3

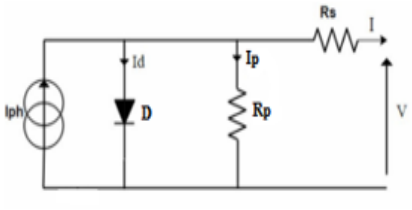

Fig. 3. Photovoltaic cell circuit.

The expression of the current I then becomes:

$$I = I_{ph} - I_0\left[exp\left(\frac{e(V + R_s I)}{\lambda K T_c}\right) - 1\right] - \frac{V + R_s I}{R_p} \quad (1)$$

Iph is a light-generated current or photocurrent [5].

PWX 500 PV module (49W) characteristics at 25 °C and 1000W/m^2 is given by table I

TABLE I. Parameters of the PV module.

Parameters	Values
P max	49 W
Imp	2.88 A
Vmp	17 V
Isc	3.11 A
Voc	21.8 V
RS	0.45 Ω
RP	310 Ω
Ns	36

Using equation 1, we were able to trace the variation curves of the I-V characteristics.

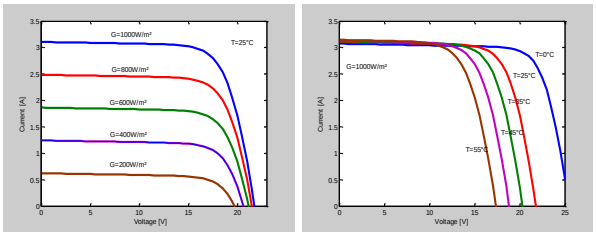

(a) (b)

Fig. 4. (a) I–V characteristics for different irradiation levels for constant T and (b) I–V different temperatures for constant irradiation.

It is found that the increase in irradiance results in a large increase in the short-circuit current but a slight increase in the open circuit voltage. On the other hand, the high temperature lowers the open circuit voltage for fixed irradiance

2.2 Converter DC/DC

The chopper is a DC/DC converter that converts DC energy at a given voltage (or current) level into DC energy at another voltage (or current) level [6].

The chopper consists of capacitors, inductors and switches [8].

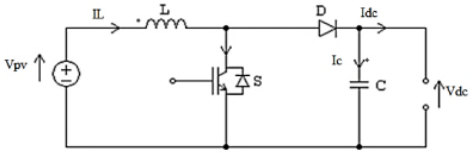

Fig. 5. Circuit diagram for Boost DC/DC converter

The inductor is used to smooth the current drawn on the source. The capacitance C is used to limit the output voltage ripple. Switch S is closed for time αT. Energy is stored in L, diode D is blocked. The blocking of S leads to the discharge of the inductor [9]. The operating principle of this type of chopper can be explained as follows:

When the switch is in position 1, the circuit is separated into two parts: on the left, the source charges the inductor, meanwhile, the capacitance on the right maintains the output voltage using the energy previously stored

2.3 Power Maximization Control

- MPPT command

By definition, an MPPT control, associated with an intermediate adaptation stage, makes it possible to operate a PV generator so as to permanently produce the maximum of its power [10].

- Disturbance and observe (P&O) command

This command is a most widely used maximum power point (PPM) tracking algorithm, and as the name suggests, it is based on the disturbance of the system by increasing or decreasing Vref or by acting directly on the duty cycle of the DC-DC converter.

Then observing the effect on the output power with a view to possible correction of this duty cycle [11].

This causes a power loss that depends on the step width of a single disturbance Cp

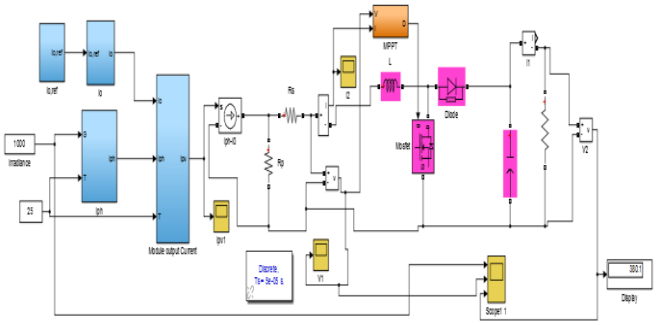

Fig. 6. PV and boost converter with MPPT

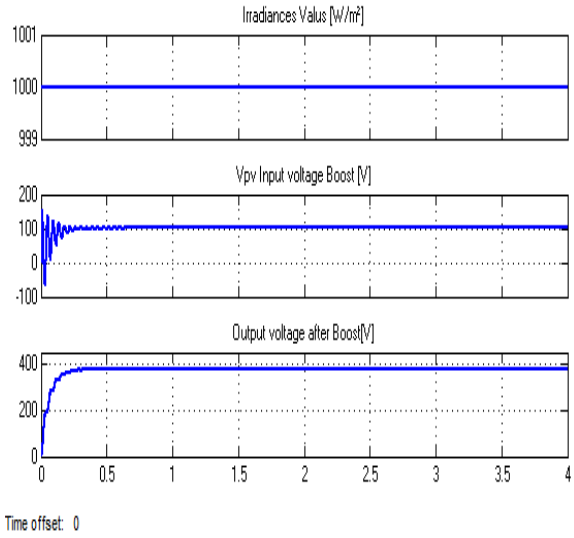

(a)

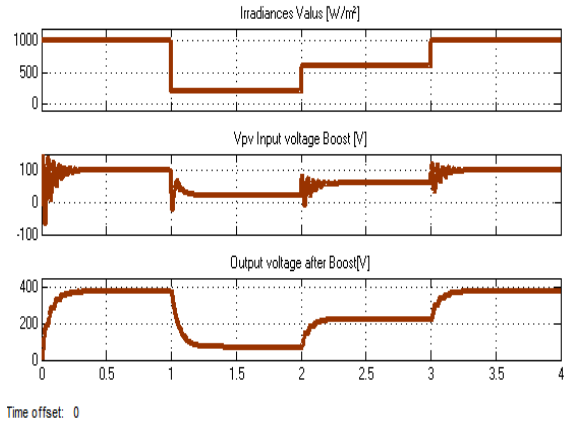

(b)

Fig. 7. Output voltage waveform of PV system

For a constant irradiance, we note the reliability of our proposed model, since the goal is to have a voltage at the output of the boost higher than that given by the photovoltaic generator which the values have been defined beforehand (V_0 = 380 V and Vs = 100 V) in Fig 7. (a).

By varying the irradiances with the bloc of Simulink Repeating Sequence Stair at Vector of output values: [1000 200 600 1000] the voltage in the load vary with the irradiances (Fig 7. (b))

2.4 Inverters (DC/AC converter)

Inverters are static circuits, which transform electrical power in direct form into power in alternating form, at a desired value of voltage or current and frequency. The output voltage of an inverter has a form periodic wave which is not sinusoidal, but which can be very close to the desired waveform [12].

The inverter obviously works with a PWM signal generation circuit controlled by a regulation circuit and protection. The latter ensures the optimal transfer of power from the solar generator to the motor pump unit and protects the pump against dry running when there is no water in the well [13].

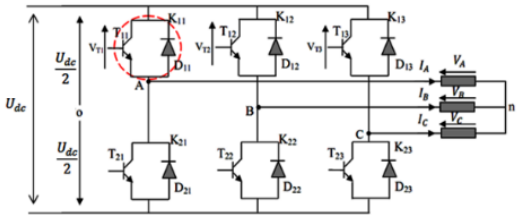

Fig. 8. Pulse width modulation (PWM) control

Among the most widely used PWM control techniques is the triangular-sinusoidal technique. It is obtained by comparing two signals, a carrier signal V_p and the reference signals V_{ref}.

Defining the logic function Sj as shown in the figure below. These logic functions associated with the control signal are defined by:

$$S_j = \begin{cases} 1 & si \quad V_{ref} \geq V_P \\ 0 & si \quad V_{ref} < V_P \end{cases} \tag{2}$$

The carrier is defined by the following formula with n: natural integer.

$$V_P = \begin{cases} \frac{4t}{T_P} - (4n+1) & si \quad t \in \left[nT_P, \left(n+\frac{1}{2}\right).T_P \right] \\ \frac{-4t}{T_P} + (4n+3) & si \quad t \in \left[\left(n+\frac{1}{2}\right).T_P, (n+1).T_P \right] \end{cases} \tag{3}$$

The reference signals are given by the following equation: avec j = 1, 2 and 3

$$V_{ref} = V_m . sin\left[(2\pi f).t - 2.(j-1).\frac{\pi}{3} \right] \tag{4}$$

In the form of Simulink blocks, the generation of pulses can be represented by the following diagram:

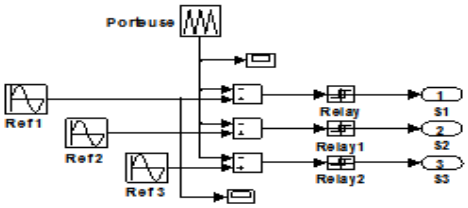

Fig. 9. The control of the inverter switch

The PWM is necessary for controlling two VSI levels of the inverter. Fig. 9 shows a comparison of two signals, which are responsible for controlling the inverter switches.

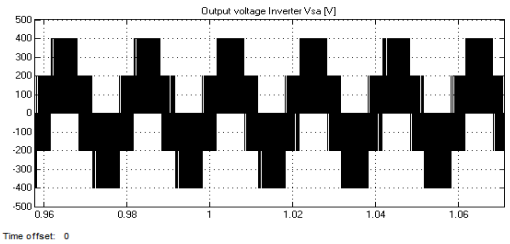

Fig. 10. Phase-to-neutral voltage at inverter output

In Fig.10, the use of sine-triangle pulse width modulation, line voltages were obtained at the output of the inverter that are not purely sinusoidal, because of the harmonics which generate losses and heating in the PV system, especially when connecting the inverter with the induction motor [13].

2.5 Model of Asynchronous motor

For a three-phase asynchronous machine supplied with voltage, the stator voltages $(V_{ds}\ V_{qs})$ and the speed of the rotating field ω_s are considered as control variables, the resistive torque Cr as disturbance. We choose in our case, the following state vector [14]:

$$X_u^T = \left(I_{ds}\ I_{qs}\ \phi_{dr}\ \phi_{qr} \right) \tag{5}$$

This choice of variable is justified on the one hand by the fact that the stator currents are measurable and on the other hand by the desire to control the norm of the rotor flux in the control law [15].

After simplification and rearrangement of the equations of the asynchronous machine in the Park frame, we obtain the model of the machine in the form of an equation of state:

$$\dot{\mathbf{X}}_u = \mathbf{A}_u\mathbf{X}_u + \mathbf{B}_u\mathbf{U} \quad (6)$$

$$A_u = \begin{bmatrix} -\lambda & \omega_s & \frac{K}{T_r} & \omega_r K \\ -\omega_s & -\lambda & -\omega_r K & \frac{K}{T_r} \\ \frac{L_m}{T_r} & 0 & -\frac{1}{T_r} & \omega_{sl} \\ 0 & \frac{L_m}{T_r} & -\omega_{sl} & -\frac{1}{T_r} \end{bmatrix}$$

$$B_u = \begin{bmatrix} \frac{1}{\sigma L_s} & 0 \\ 0 & \frac{1}{\sigma L_s} \\ 0 & 0 \\ 0 & 0 \end{bmatrix} U = \begin{bmatrix} V_{ds} \\ V_{qs} \end{bmatrix} \quad (7)$$

With:

$$T_r = \frac{L_r}{R_r}, K = \frac{L_m}{\sigma L_s L_r}, \sigma = 1 - \frac{L_m^{\ 2}}{L_r L_s}, \lambda = \frac{R_s}{\sigma}.\frac{1}{L_s} + \frac{L_m^{\ 2}}{\sigma}.\frac{R_r}{L_s.L_r^{\ 2}}$$

The complete model of the system is given by this equation [16]:

$$C_e = \frac{3}{2} p \frac{M}{L_r}(\phi_{dr} I_{qs} - \phi_{qr} I_{ds}) \quad (8)$$

$$\frac{d\Omega_r}{dt} = (C_e - C_r - f_r \Omega_r)/J$$

Then the model of the MAS supplied with voltage is found with 5 equations (2 magnetic + 2 electrical + 1 mechanical)

This mathematical model of MAS can be put under a Simulink scheme based on "Fcn" blocks, integrators and 'Mux'. The Simulink block diagram of the motor can be reduced to a single block where the inputs are the three-phase supply voltages and the mechanical load, while the outputs are the stator currents, rotor flux, electromagnetic torque, and speed [17].Parameters of this motor are given in Table II.

TABLE II. Asynchronous machine parameters

Power:	P=1.5kw
Voltage	U=380/220V
Frequency:	f=50Hz
Rotation speed	N=1450rpm
Number of pole pairs	p=2
Stator resistance:	Rs=4.85Ω
Rotor resistance	Rr=3.81Ω
Stator inductance	Ls=0.274H
Rotor inductance	Lr=0.274H
Mutual inductance:	Lm=0.258H
The moment of inertia:	J=0.031kg.m^2
The coefficient of friction	fr=0.0114N.m/rd/s.

2.6 The centrifugal pump

The operating theory of centrifugal pumps shows that between the inlet and the outlet of the impeller, the total mechanical energy of the fluid stream is increased, this increase comes from an increase in the pressure energy on one hand and also an increase in the kinetic energy, the latter is transformed into pressure energy by progressively slowing down which is obtained in a part placed inside the wheel called cochlea, this one ends in a divergent cone [18].

The centrifugal pump is mainly characterized by a resisting torque, which is of the following form:

$$Cr = kp.\omega^2 \quad (9)$$

Where:

kp: Proportionality coefficient [Nm/ (rad.s-1)²]

ω: Angular velocity [rad.s-1]

With:

$$kp = \frac{Pm}{\omega^3} \quad (10)$$

- Power calculation:

A pump is a machine that supplies energy to a fluid in order to move it from one point to another. The general expression of the hydraulic power is given as follows:

$$Ph = \rho.g.Q.H \quad 11)$$

Ph is the power that the pump transmits to the fluid W (watt)

The other expression considered is that of the power absorbed by a pump, i.e. the power required for its mechanical drive, which is expressed by the following relationship:

$$Pm = 9.81.\rho.H.\frac{Q}{\eta p} \quad (12)$$

With

Pm: Mechanical power of the engine

H is the total height (m)

ηp : pump performance

ρ: Density of water (1000Kg/ m3)

Q: Flow (m3/s)

- Yield calculation:

$$\eta m = \frac{P_H}{Pa} \qquad (13)$$

For electric pump sets (pump + motor), manufacturers generally give the overall efficiency curve.

The water flow related to the mechanical power absorbed by the pump is given by the following relationship:

$$Q = \frac{Pm.\eta_p}{\rho.g.H} \qquad (14)$$

If we assume that the efficiency of the coupling is equal to one, then the mechanical power of the motor (useful) is equal to the power absorbed by the pump. Knowing the efficiency of the motor, the electrical power absorbed by the motor is:

$$Pa = \frac{Pu}{\eta_m} \qquad (15)$$

Where aldehydePu is motor power and η_m is motor efficiency

3. Simulation Of The Global Chain

To test the proper functioning of all the elements of the system, the Simulink environment was used, the block diagram is represented as follows (Fig.11)**.**

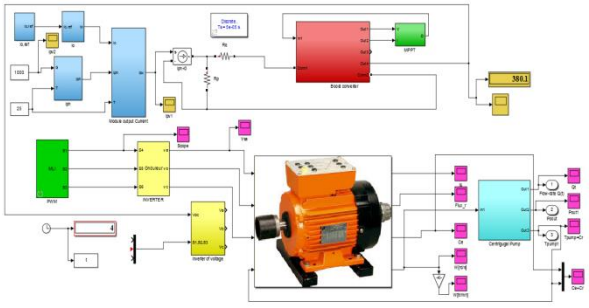

Fig 11. Block diagram of the photovoltaic pumping system using MATLAB/Simulink

The squirrel-cage asynchronous motor has several advantages in their simplicity of construction and maintenance, their mechanical robustness and their low cost price. It is very commonly used in a power range from a few hundred watts to several thousand kilowatts. This motor is characterized by stable operation, nearly constant speed and high efficiency around the rated load [18].

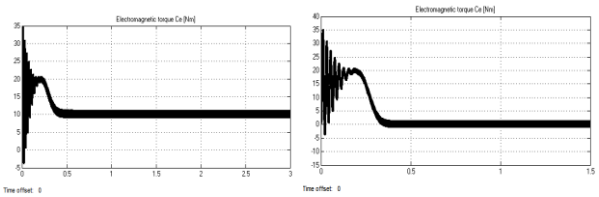

(a) (b)

Fig 12. Electromagnetic torque Evolution (N.m)

In idle mode without the pump Fig.12 (a), the evolution of the torque in the first time is a typical characteristic of all squirrel-cage induction motors. This one presents at the first moments pulsations very important. During the transient regime, the torque is strongly pulsating, and then stabilizes at the end of the regime, in the load regime Fig.12 (b).

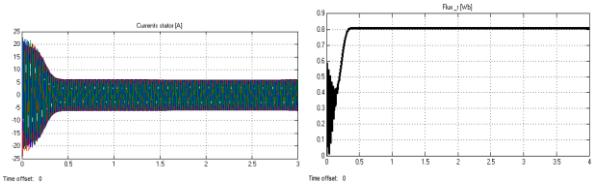

(a) (b)

Fig 13:.Evolution of the stator currents and the rotor Flux

On starting, the motor current is limited within authorized limits from which there is a soft start in Fig.13 (a), the rotor flux is given by Fig.13 (b).

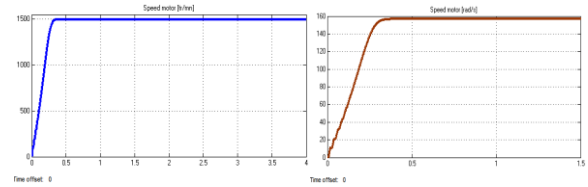

Fig 14. Speed Waveform of Asynchronous Motor

After the simulation, it was noticed that the rotational speed of the asynchronous motor would evaluate over time and reach its nominal speed (156 rad/s or 1500 rpm) in a slow time, with a tendency to oscillate due

to the inertia of the rotating masses and the damping coefficient due to the low flux values, in Fig.14.

It is clear from the figure below that the speed of the asynchronous motor is constant without any oscillation. The motor is controlled by V/f control technique. The speed of the motor depends on the frequency of the supply voltage.

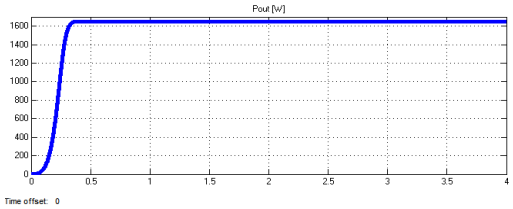

Fig. 15. Motor output power (Pout)

In Figure 15, we can see the evolution of the Pout of the motor with the pump as charge. this power absorbed by the motor of the order of 1650 Watt, which is greater than its mechanical power (1500 Watt). The power to be supplied by the photovoltaic generator will be determined by the nominal power requested by the motor-pump assembly

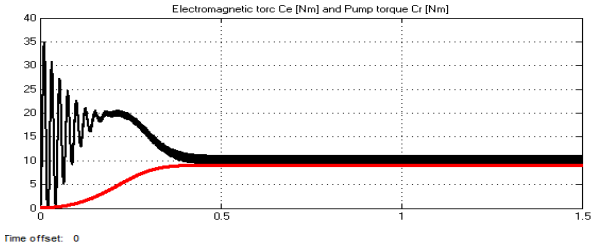

Fig 16. Electromagnetic torque Ce and resistive torque Cr (pump).

The electromagnetic torque perfectly follows the torque pump resistant

The starting and steady state behavior of the motor+pump at 1000 W/m^2 are shown in Figure. 16. All motor indexes such as the speed N, the electromagnetic torque Ce and the load torque offered by the pump Cr reach their nominal values under steady state conditions because the MPP is followed. A small pulsation of Ce results from the electronic switching of the motor

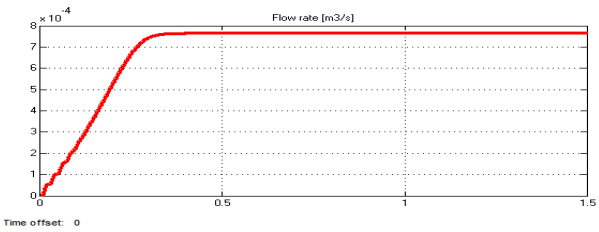

Fig. 17. Shows the evolution of the flow rate of the pump

Figure 17 shows the evolution of the flow rate. The water flow sees its value reach 7.8 x 10^{-4} m^3/s of the pump. It can be seen that MPPT techniques have in P&O shows that losses due to motor efficiency are system losses.

By varying the irradiances in the last Fig.18, we can show the evolution of the stator currents in Fig.19.

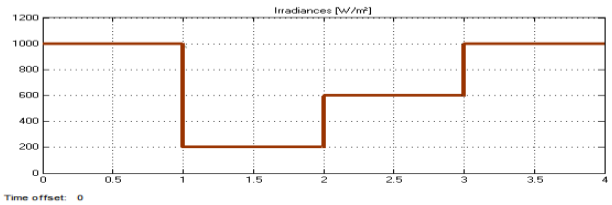

Fig 18: Solar radiation and stator currents

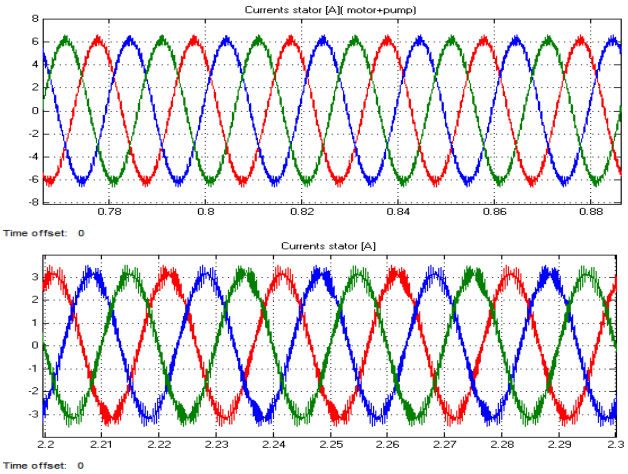

Fig. 19. Zoom of the stator currents for two different irradiances

The motor draws its rated current of 6.1A at G=1000 W/m² and 3.4A at G=600 W/m²A and achieves its rated speed of 1500 rpm, driving water pumping at full capacity. It can be seen that the current is dependent on the increase or decrease in irradiation

4. Conclusion

In this work, it is a question of modeling, simulating a photovoltaic generator associated with a DC-DC converter controlled by MPPT, intended to control an asynchronous machine through a DC-AC converter supplying in last a centrifugal pump. To do this, we started with a general study on photovoltaic conversion, followed by the development of a mathematical model for the PV panel based on a circuit equivalent to a diode. At the end of the simulations carried out, we noted a strong

dependence of the performances of the photovoltaic module according to the climatic conditions, in particular the irradiance and the temperature of the module. The role of interface between the two elements by ensuring, by a regulating action, the transfer of the maximum power supplied by the generator so that it is as close as possible to the maximum power. The second part of this work was the subject of sizing of DC-DC converters commonly used in photovoltaic conversion chains. The output is transformed into alternating voltages thanks to an inverter controlled by a PWM thus feeding an asynchronous motor and as a load; we have inserted a centrifugal pump.

The solar PV panel-based asynchronous motor water pumping system using DC-DC step-up converter has been proposed and its applicability has been confirmed by performance evaluations under practical operating conditions. Therefore, we can propose the integration of this system for pumping water as a feasible solution in a context of simplicity, efficiency, reliability and availability.

References

[1] Tijjani Baraya, J., Hamza Abdullahi, B., Sylvester Igwenagu, U. (2020). The effect of humidity and temperature on the efficiency of solar power panel output in Dutsin-ma local government area (L.G.A), Nigeria. Journal of Asian Scientific Research, 10(1): 1-16. https://doi.org/10.18488/journal.2.2020 20.101.1.16

[2] N. Femia, G. Petrone, G. Spagnuolo, M. Vitelli, Power Electronics and Control Techniques for Maximum Energy Harvesting in Photovoltaic Systems. CRC Press: Boca Raton, 2013, pp. 42–45.

[3] Motahhir, S.; El Hammoumi, A.; El Ghzizal, A. Photovoltaic system with quantitative comparative between an improved MPPT and existing INC and P&O methods under fast varying of solar irradiation. Energy Rep. 2018, 4, 341–350.

[4] Saidi, K.; Maamoun, M.; Bounekhla, M. A new high performance variable step size perturb-and-observe MPPT algorithm for photovoltaic system. Int. J. Power Electron. Drive Syst. 2019, 10, 1662–1674.

[5] Ozdemir, S., Altin, N., Sefa, I., & Bal, G. (2014). PV Supplied Single Stage MPPT Inverter for Induction Motor Actuated Ventilation Systems. Elektronika Ir Elektrotechnika, 20(5), 116-122. https:// doi.org/10.5755/j01.eee.20.5.7111

[6] Song, X., Yuan, C., Zhang, Y., Li, Q., & Li, Z. (2018). A New Numerical Modelling Method for System Energy Efficiency Calculation. Elektronika Ir Elektrotechnika, 24(6), 55-59. https://doi.org/10.5755/j01. eie.24.6.21520

[7] Sh. Biswas and M. T. Iqbal, “Dynamic modelling of a solar water pumping system with energy storage”, Hindawi Journal of Solar Energy, vol. 2018, article ID 8471715, pp. 1–12, 2018. DOI: 10.1155/2018/ 8471715.

[8] A. Al-Badi and H. Yousef, “Design of photovoltaic water pumping system as an alternative to grid network in Oman”, Renewable Energy and Power Quality Journal (RE&PQJ), no. 14, pp. 11–15, 2016. DOI: 10.24084/repqj14.203.

[9] Khelifa Khelifi Otmane” Anti windup GPC speed controller for induction machine based on Youla parametrization” Journal of Electrical Engineering, Vol 73, 1 (2022) 50-56, https://doi.org/10.2478/jee-2022-0007.

[10] Chung Mai Van – Sang Duong Minh – Duc Tran Huu – Bao Binh Pho – Phuong Vu” An improved method of model predictive current control for multilevel cascaded H-bridge inverters” Journal of Electrical Engineering, Vol 72, 1 (2021) 1-11 https://doi.org/10.2478/jee-2021-0001

[11] J. Liang et al. “Evolutionary multi-task optimization for parameters extraction of photovoltaic models,” Energy Convers. Manag., Vol. 207, p. 112509, 2020

[12] F. A. Hashim, E. H. Houssein, K. Hussain, M. S. Mabrouk, and W. AlAtabany, “Honey Badger Algorithm: New metaheuristic algorithm for solving optimization problems,” Math. Comput. Simul., Vol. 192, pp. 84-110, 2022

[13] Y. Agrebi, Y. Koubaa and M. Boussak “Online Rotor ResistanceEstimation Using the Model Reference Adaptive System of Induction Motor”, i-manager’s Journal of Electrical Engineering, vol. 3 no 3 January- March 2010.

[14] Y. Xing, “A novel rotor resistance identification method for an indirect rotor flux-oriented controlled induction machine system,”. IEEE Trans. Power Electron., vol. 17, pp. 353–364, 2002

[15] S. Jain, A.K. Thopukara, R. Karampuri and V.T. Somasekhar, "ASingle-Stage Photovoltaic System for a Dual-Inverter-Fed Open-End Winding Induction Motor Drive for Pumping Applications," IEEE Transactions on Power Electronics, vol. 30, no. 9, pp. 4809 - 4818, Sept. 2015.

[16] B. Singh and V. Bist, "A BL-CSC Converter-Fed BLDC Motor Drive with Power Factor Correction," IEEE Transactions on Industrial Electronics, vol. 62, no. 1, pp. 172-183, Jan. 2015.

[17] Wang, F.; Zhang, Z.; Mei, X.; Rodríguez, J.; Kennel, R. Advanced control strategies of induction machine: Field oriented control, direct torque control and model predictive control. Energies 2018, 11, 120

[18] Ramani R. , Nalini A. ''Analysis of DC-DC Converter for Energy Management in Electric Vehicle''Journal of Harbin Engineering University, Vol. 44 No. 11 (2023): Issue 11.